光学学报

基于原子层沉积技术的X射线多层膜的制备研究

吕文思[1,2]，吴宏昌[1,3]，李艳丽[1*]，孔祥东[1,2**]，韩立[1,2]
[1]中国科学院电工研究所，北京 100190；
[2]中国科学院大学电子电气与通信工程学院，北京 100049；
[3]兰州大学物理科学与技术学院，甘肃 兰州 730000

摘要 X射线多层膜是X射线光学领域的重要反射元件，可利用X射线的布拉格反射实现特定波段X射线的高效反射。多层膜的反射率与膜层材料和膜层结构密切关系，根据多层膜的工作原理，对于高能波段的X射线，为获得较大掠射角下的高反射率，通常需要多层膜具有更小的周期厚度和更大的周期数，因此高精度薄膜生长技术是X射线多层膜元件制备的必要条件。本文研究了基于原子层沉积技术的X射线多层膜的制备，首先利用Fresnel系数递推法计算出HfO_2/Al_2O_3、Ir/Al_2O_3、Ru/Al_2O_3、W/Al_2O_3四种材料组合的多层膜的反射率，讨论了材料组合、周期厚度、周期数、占空比等参数对多层膜反射率的影响。在此基础上，选取并制备了周期厚度为4 nm、周期数为60、占空比为0.5的HfO_2/Al_2O_3 X射线多层膜。X射线(0.154 nm)反射率的分析结果显示，该多层膜的周期厚度为3.86 nm，反射率约43%，多层膜截面的透射电子显微镜(TEM)图显示膜层间界面清晰。该结果验证了原子层沉积法制备小周期厚度X射线多层膜元件的可行性。

关键词 原子层沉积；X射线；多层膜；反射率
中图分类号 O434.1 **文献标志码** A **DOI**: 10.3788/AOS231331

1 引 言

X射线光学元件是应用于X射线波段的元件，广泛应用于同步辐射与自由电子激光、高能天文观测、实验室X射线检测等大科学装置或X射线仪器中[1]，主要包括X射线波带、毛细管、反射镜、光栅等[2-7]。其中，X射线多层膜是一类重要的反射元件，通常由两种高、低原子序数材料交替组成，利用多个界面反射光的相干叠加，实现特定波段X射线的高效反射。X射线多层膜具有反射率高、工作角度大等特点，已被广泛应用于前沿科学研究和重大科学设施中。

多层膜的工作原理是利用X射线的布拉格反射，由于X射线的波长短(0.01~10 nm)，所以多层膜的周期厚度通常在几到几十纳米量级，且在入射角不变的情况下，多层膜的周期厚度随X射线波长的减小而减小。当多层膜的周期厚度降到几纳米时，多层膜的缺陷会导致X射线反射率的大幅降低，包括膜层界面间的扩散、薄膜粗糙度等[8]，因此，小周期厚度X射线多层膜的制备离不开高精度的薄膜制备技术。

目前，X射线多层膜的制备方法主要是离子束溅射技术、磁控溅射技术、原子层沉积技术等。离子束溅射技术镀膜速率稳定、易于控制参数、薄膜结构紧密，王国田等[9]运用离子束溅射技术制备了周期厚度为15 nm、周期数为31的C/Si多层膜结构，在波长30.4 nm和28.4 nm附近反射率分别可达到14%和11%左右，由于离子束溅射制备的薄膜的高均匀性极大程度上依赖于制备过程中良好的真空环境，因而真空度不达标时会生成低质量薄膜，难以拥有预期的光学特性[10]。磁控溅射技术工艺稳定，是目前X射线多层膜元件的主要制备方法[11-16]，张云学等[17]已运用磁控溅射技术在高精度Si基底上分别镀制了W/Si多层膜和Ru/C多层膜，周期厚度为3 nm，周期层数分别为70和75，X射线(0.154 nm)反射率分别为63%和62%，但是磁控溅射的设备庞大复杂、价格昂贵。原子层沉积(ALD)技术为一种气相化学反应，利用两种或多种反应物为前驱体，在目标基体上以表面自限制生长模式交替反应，实现目标薄膜的单原子层生长，薄膜厚度控制精度在埃米量级，具有自限制性、高保形性以及埃米量级的薄膜厚度控制精度，在制备小周期厚度多层膜方面具有巨大潜力。吴鹿杰等[4]利用ALD法制备了Al_2O_3/HfO_2多层结构，单层膜厚度为10 nm；Fabreguette团队[18-19]运用ALD技术制备了周期数为16、周期厚度为10 nm的W/Al_2O_3多层膜，反射率测量结果显示多层膜具有很高的反射率，由于周期

收稿日期：2023-07-31；**修回日期**：2023-10-18；**录用日期**：2023-12-12；**网络首发日期**：2023-12-23
基金项目：国家自然科学基金(12104454)、中国科学院电工研究所基金(E1554404)
通信作者：*liyanli@mail.iee.ac.cn；**slkongxd@mail.iee.ac.cn

厚度大，高能X射线(0.154 nm)的掠射角很小。

本文研究利用ALD法制备更小周期厚度的X射线多层膜，根据ALD可制备的薄膜类型，计算了4种膜系多层膜的X射线反射率，包括HfO_2/Al_2O_3、Ir/Al_2O_3、Ru/Al_2O_3和W/Al_2O_3，并进一步分析了多层膜结构参数对反射率的影响，在此基础上利用ALD法制备了周期数为60、周期厚度为4 nm、占空比为0.5的Al_2O_3/ HfO_2多层膜。测试结果显示，多层膜的膜层间界面较清晰，并具有较高的X射线反射率。

2 实验过程和测试方法

2.1 实验过程

本文使用的ALD设备为嘉兴科民T-ALD 150D型原子层沉积系统，其中氧化铝和氧化铪薄膜所用的金属前驱体分别为三甲基铝(TMA)和四(二甲胺基)铪(TDMAH)，氧源为去离子水，载气为纯度为99.999%的高纯氮气，多层膜的基底为直径为6.67 cm的单晶硅(表面粗糙度约为5 Å)。薄膜制备过程中TDMAH源加热至75 ℃，反应腔体上下底板加热温度为150 ℃，管路温度为120 ℃，腔体压强为26.67 Pa。Al_2O_3薄膜的一个循环过程包括通入前驱体TMA 0.015 s，N_2吹扫30 s，通入氧源去离子水0.02 s后，N_2吹扫30 s。HfO_2薄膜的一个循环过程包括通入前驱体TDMAH 0.02 s，反应10 s，N_2吹扫40 s，通入氧源去离子水0.03 s，反应10 s后，N_2吹扫40 s。图1为镀制结束后的多层膜结构示意图，最终形成了周期厚度为4 nm的Al_2O_3/HfO_2多层膜，其每个周期厚度中Al_2O_3与HfO_2的循环数分别设置为8和12，总周期数为60。

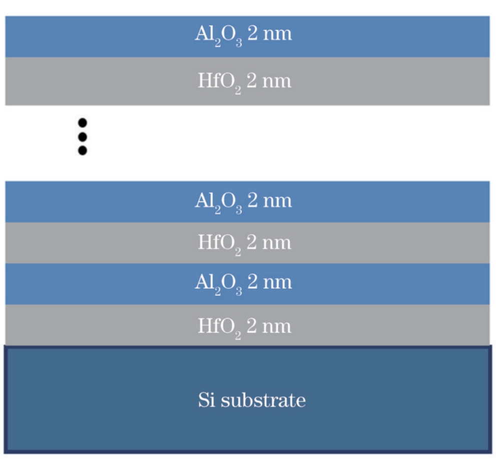

图1 HfO_2/Al_2O_3多层膜的结构示意图

Fig. 1 Structure diagram of HfO_2/Al_2O_3 multilayers

2.2 测试方法

所制备的样品经美国ThermoFisher公司Scios 2型聚焦离子束电子束(FIB-SEM)系统提取出垂直样品表面的截面薄片样品，并利用微机械臂将截面样品转移到透射电子显微镜(TEM)专用载网上，通过离子束进一步减薄抛光后利用日本电子JEM-2100F型TEM观察多层膜的结构；多层膜的反射率在北京同步辐射1W1A线站上测试，X射线波长为0.154 nm，测试前将样品置于水平样品台上，在调整好样品台、探测器等的位置后，设置扫描角度范围，获得不同掠射角下X射线的强度值，并利用IMD软件拟合，分析获得X射线的反射率。

3 X射线多层膜理论

3.1 多层膜结构

X射线多层膜通常是由两种材料交替镀制成，一层由高原子序数的材料(材料1)组成，作为散射层可以实现对X射线的散射；另一层由低原子序数材料(材料2)组成，作为间隔层，起支撑作用。多层膜的反射率可利用基于Fresnel公式的光学多层膜理论进行计算[20-23]，在复折射率为$\tilde{n}_0=n_0-\mathrm{i}\beta_0$的无限厚基片上，如图2中多层膜反射率的计算示意图所示，在基底上依次生长厚度为d_j($j=1, 2, 3, \cdots, m$)的薄膜，膜层折射率为$\tilde{n}_j=n_j-\mathrm{i}\beta_j$，波长为$\lambda$的平行光从空气以$\theta$角掠入射到多层膜表面，理想界面情况下，$m$层多层膜中的第$j$层Fresnel反射率系数为

$$r_j=\frac{r_{j-1,j}+r_{j-1}\exp(\mathrm{i}2\delta_j)}{1+r_{j-1,j}r_j\exp(\mathrm{i}2\delta_j)},\tag{1}$$

$$\tilde{n}_0\cos\theta=\tilde{n}_j\cos\theta_j,\tag{2}$$

式中：相位差$\delta_j=2\pi d_j\tilde{n}_j\sin\theta_j/\lambda$；$\theta_j$为第$j$层的入射角；$\lambda$为入射光波长；$r_{j-1,j}$为第$j-1$层和第$j$层之间的Fresnel反射系数。从$j=1$起直到$j=m$作迭代计算得到多层膜反射系数，最终可得多层膜的反射率。

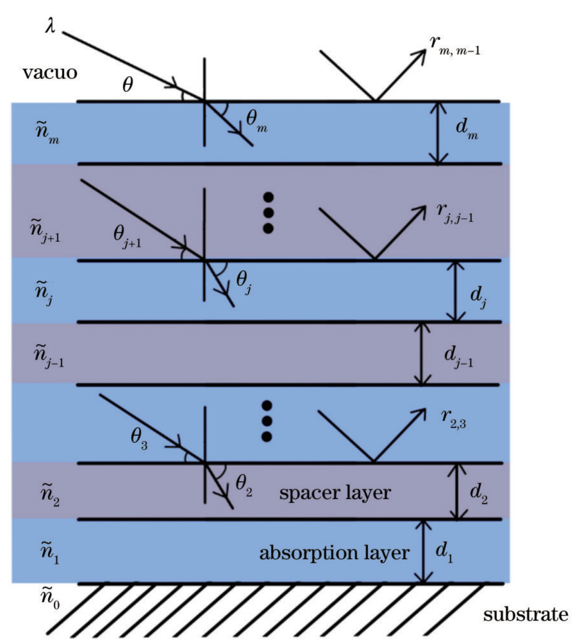

图2 多层膜的反射率计算示意图

Fig. 2 Diagram of reflectance calculation for multilayers

为了尽可能提高多层膜的反射率，组成多层膜材料的选取应满足：两种材料的折射率差别尽可能大；两种材料在工作波段的吸收尽可能小；从而实现两种材料形成的 Fresnel 反射系数差尽可能大。所以当X射线以 θ 角度掠入射进入多层膜时，发生类似布拉格衍射效应，X射线在多层膜表面发生布拉格振荡，实现X射线的高反射，对于周期性多层膜结构则有布拉格公式为

$$m\lambda = 2(d_1 + d_2)\sqrt{\frac{n_1 d_1 + n_2 d_2}{d_1 + d_2} - \cos^2\theta}, \quad (3)$$

式中：散射层材料1的厚度为 d_1，折射率为 n_1；间隔层材料2的厚度为 d_2，折射率为 n_2；m 为衍射级次；λ 为X射线的波长，多层膜周期厚度为 $D=d_1+d_2$，则可以根据其选择镀制多层膜的不同材料。此外，两种材料能形成连续的膜层，且膜层间界面光滑、相互扩散小，两种材料不发生相互反应，界面粗糙度尽可能小。X射线多层膜的主要参数包括膜层材料、周期厚度 $D(d_1+d_2)$、占空比 $\tau(d_1/D)$ 和周期数 N，下面依次分析这些参数对X射线反射率的影响。

3.2 膜层材料对反射率的影响

ALD法可制备多种薄膜材料，可作为多层膜散射层的薄膜包括 W、Ir、Ru、HfO_2 等，可作为多层膜间隔层的薄膜包括 Al_2O_3、SiO_2 等，根据 Fresenel 系数递推分别计算了 $D=4$ nm、$\tau=0.5$、$N=100$ 的 HfO_2/Al_2O_3、Ir/Al_2O_3、Ru/Al_2O_3 和 W/Al_2O_3 四种膜系多层膜的X射线（0.154 nm）反射率，如图3所示，可以看出，四种多层膜的一级衍射峰位置相差不大，在1.1°～1.2°之间，其位置主要是由周期厚度 D 所决定的，对于 $D=4$ nm、$\tau=0.5$、$N=100$ 的四种多层膜，发生一级衍射时X射线的理论反射率均高于50%，其中 Ir/Al_2O_3、Ru/Al_2O_3 和 W/Al_2O_3 多层膜的最高理论反射率基本相同，约为71%，HfO_2/Al_2O_3 多层膜的峰值反射率略低，约为55%，这主要是因为相比于其他三种金属膜，HfO_2 与 Al_2O_3 在0.154 nm X射线处的折射率差别较小。

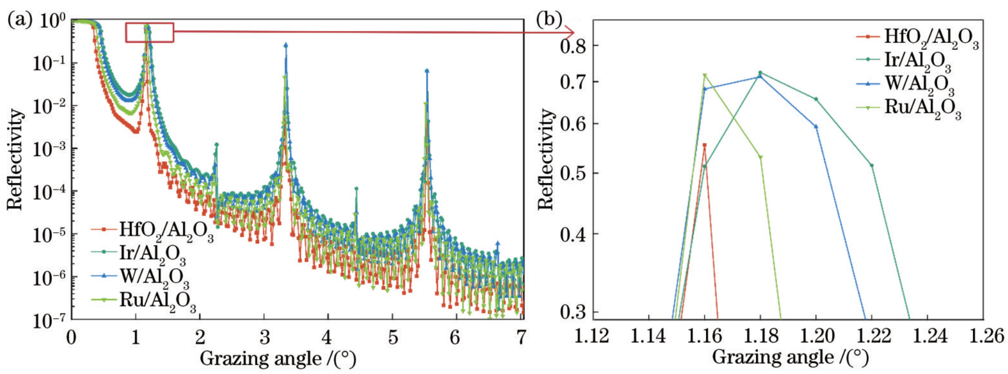

图3 不同膜系多层膜反射率与X射线掠射角度的关系。(a)在掠射角为0°到7°时不同膜系多层膜反射率的变化；(b)在一级衍射峰处的不同膜系多层膜的反射率

Fig. 3 Relationship between reflectivity of multilayer films of different film systems and grazing angle of X-rays. (a) Changes in reflectivity of multilayer films of different film systems at grazing angles from 0° to 7°; (b) reflectivity of multilayer films of different film systems at primary diffraction peak

3.3 周期厚度 D 对反射率的影响

以 $\tau=0.5$、$N=100$ 的 HfO_2/Al_2O_3 多层膜为例，计算了不同周期厚度多层膜的X射线（0.154 nm）反射率与掠射角的关系，如图4所示。可以看出，多层膜一级衍射峰出现时的掠射角随着周期厚度的增加而减小，这也是符合式(2)的计算规律。同时也可以看到，同样占空比和周期数下，X射线的最高反射率不同，这是膜层厚度影响Fresnel反射率系数的结果。

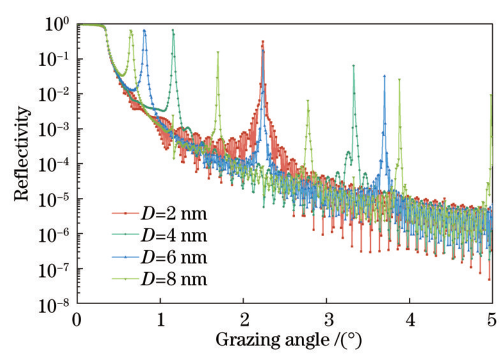

图4 不同周期厚度的 HfO_2/Al_2O_3 多层膜反射率与X射线掠射角度的关系

Fig. 4 Relationship between reflectivity of HfO_2/Al_2O_3 multilayer films with different periods and grazing angle of X-rays

3.4 占空比 τ 对反射率的影响

以 $D=4$ nm、$N=100$ 的 HfO_2/Al_2O_3 多层膜为例，发生一级衍射时X射线（0.154 nm）反射率与占空比的关系，如图5所示。从图中可以看出，反射率随占空比的增加呈现先增加后饱和最后降低的变化趋势，这是 HfO_2 层对X射线调制过程的结果，随着 HfO_2 厚度的增加，它对X射线的调制作用增强，当占空比 τ 在0.4～0.5之间时，X射线的反射率较高，随着 HfO_2 厚度的增加，它对X射线的吸收起主要作用，导致反射率下降。

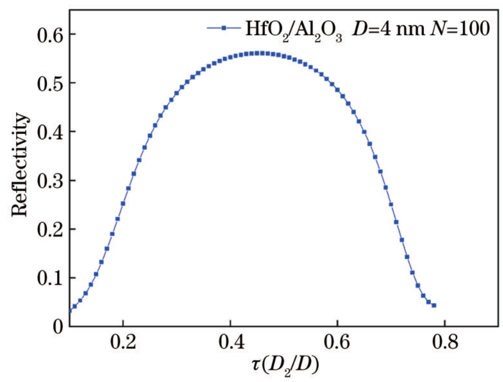

图5 HfO_2/Al_2O_3多层膜反射率随占空比的变化曲线

Fig. 5 Variation of reflectivity of HfO_2/Al_2O_3 multilayers with duty ratio

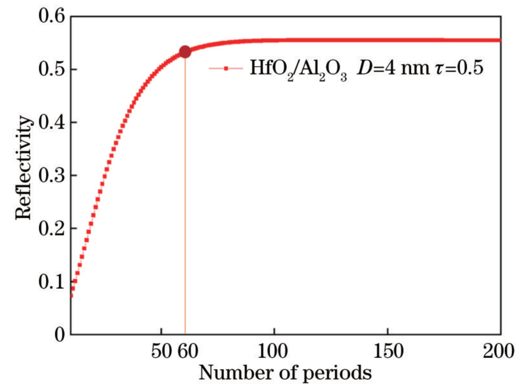

图6 HfO_2/Al_2O_3多层膜反射率随周期数的变化曲线

Fig. 6 Variation of reflectivity of HfO_2/Al_2O_3 multilayers with number of periods

3.5 周期数 *N* 对反射率的影响

以$D=4$ nm、$\tau=0.5$的HfO_2/Al_2O_3多层膜为例，发生一级衍射时X射线（0.154 nm）反射率与周期数的关系，如图6所示。可见，X射线反射率随着周期数的增加而增加，呈现出先快速增长后趋于饱和的变化趋势。这主要是因为周期数增加后，反射X射线的界面数增加，进而增加相干叠加的X射线。但反射率增加程度是X射线反射、吸收及透射三种因素相互竞争的结果，随着周期数N的增加，存在着一个饱和值，当N进一步增加时，多层膜已经不能被X射线穿透，反射率也几乎保持不变。 可以看到，当$N<60$时，反射率随周期数快速增长，当$N>60$后，反射率的增长速度变缓，$N=60$的HfO_2/Al_2O_3多层膜的反射率约为53%，略低于最高反射率55%，但周期数比饱和周期数（100）少40时，制备时间更短，所以本文制备周期数为60的HfO_2/Al_2O_3多层膜。

4 测试结果与分析

4.1 TEM测试结果

图7为不同放大倍率下HfO_2/ Al_2O_3多层膜截面的TEM图，HfO_2层是较暗的区域，Al_2O_3层则是较亮的区域，因为相对于Al元素，Hf的原子序数大，对电子的散射更强，图中有些条状区域看不清多层膜结构，这主要是因为FIB减薄样品过程中的窗帘效应所致，样品表面有微小起伏，导致不同位置的焦距略有不同。从图中可以看出，HfO_2和Al_2O_3的界面较清晰，但同时可以看到，在一个周期中，HfO_2的厚度略大于Al_2O_3的厚度，表明膜层间存在一定的扩散，尤其是当HfO_2长在Al_2O_3层上时，由于Al_2O_3的密度小于HfO_2的密度，HfO_2的分子质量大，动能大，HfO_2可能更容易渗透到Al_2O_3的空隙中，导致HfO_2厚度的增加，类似的扩散现象也出现在Nb/Si[24]、Mo/Si[25]、Mo/Al[26]等多层膜体系中。

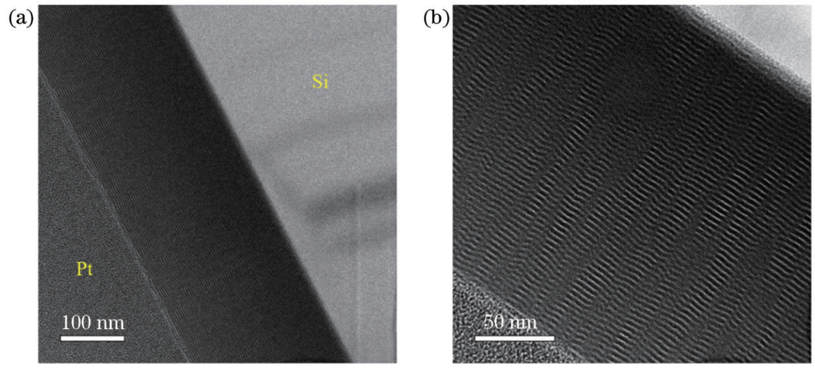

图7 HfO_2/Al_2O_3多层膜截面的TEM图。(a)50层HfO_2/Al_2O_3堆叠薄膜的TEM图；(b)放大后的TEM图

Fig. 7 Cross-sectional TEM images of HfO_2/Al_2O_3 multilayers. (a) Cross-sectional TEM image of 50 layers HfO_2/Al_2O_3 stack films; (b) TEM image after magnification

4.2 X射线反射率测试结果

多层膜X射线的反射率测试结果和IMD拟合结果如图8所示，从图中可以清晰地看到，两级布拉格衍射峰分别位于1.15°和2.23°处，衍射峰的宽度较小，这也表明薄膜沉积速率稳定，多层膜中各个周期的厚度相差不大。通过分析拟合数据，得到多层膜的$D=3.86$ nm（其中Al_2O_3层为1.91 nm，HfO_2层为1.95 nm），反射率为43%，低于理论的最高反射率

55%。分析其原因,主要源自于基底Si和多层膜的粗糙度、膜层间的微小扩散等因素,其中基底的粗糙度会累积传递给多层膜,进而导致X射线的散射增加,反射率下降。通过IMD软件计算,对于膜层粗糙度为5 Å、D=4 nm、N=60、τ=0.5 的 HfO_2/Al_2O_3 多层膜,0.154 nm X射线的最高反射率降至45%,因此,通过减小基底粗糙度来降低膜层粗糙度有望进一步提高X射线的反射率。

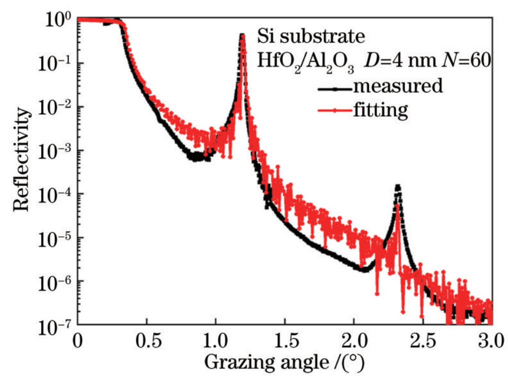

图8 HfO_2/Al_2O_3多层膜的X射线反射率测量结果和拟合结果

Fig. 8 X-ray reflectivity measurement and fitting results of HfO_2/Al_2O_3 multilayers

5 结 论

本文采用ALD技术制备了X射线多层膜,计算了理想情况下不同膜层材料、不同结构参数下多层膜的X射线(0.154 nm)反射率,并详细讨论了膜层材料、周期厚度、周期数和占空比对反射率的影响。计算结果显示,D=4 nm、τ=0.5、N=60 的 HfO_2/Al_2O_3 多层膜具有53% 的理论最高反射率,在此基础上,利用ALD法制备出该HfO_2/Al_2O_3多层膜。多层膜TEM测试结果显示,膜层间的界面较清晰,X射线反射率测试结果表明,多层膜具有43% 的一级衍射效率,这也证实了ALD法制备小周期厚度X射线多层膜元件的可行性和巨大潜力。

参 考 文 献

[1] 黄秋实, 齐润泽, 张哲, 等. 高性能大尺寸X射线多层膜反射元件研制进展[J]. 光学 精密工程, 2022, 30(21): 2793-2804.
Huang Q S, Qi R Z, Zhang Z, et al. Development of high performance and large size X-ray multilayer reflective optics[J]. Optics and Precision Engineering, 2022, 30(21): 2793-2804.

[2] Wang H C, Moriconi S, Sawhney K. Nano-precision metrology of X-ray mirrors with laser speckle angular measurement[J]. Light: Science & Applications, 2021, 10: 195.

[3] 陈宜方. 电子束光刻研制高分辨X射线波带片透镜最新进展[J]. 光学学报, 2022, 42(11): 1134005.
Chen Y F. Recent progress in nanofabrication of high resolution X-ray zone plate lenses by electron beam lithography[J]. Acta Optica Sinica, 2022, 42(11): 1134005.

[4] 吴鹿杰, 文庆涛, 高雅增, 等. 基于原子层沉积技术的高精度多层膜X射线菲涅尔波带片的制备研究[J]. 光子学报, 2021, 50(1): 0123001.
Wu L J, Wen Q T, Gao Y Z, et al. Investigation on the preparation of high precision multilayer X-ray Fresnel zone plates based on atomic layer deposition technology[J]. Acta Photonica Sinica, 2021, 50(1): 0123001.

[5] 孙天希. 毛细管X射线透镜技术及其应用[J]. 光学学报, 2022, 42(11): 1134002.
Sun T X. Capillary X-ray lens technology and its applications[J]. Acta Optica Sinica, 2022, 42(11): 1134002.

[6] 谭明生, 明帅强, 吴雨菲, 等. 原子层沉积与聚焦离子束切片法制备X射线波带片[J]. 光学学报, 2023, 43(11): 1134001.
Tan M S, Ming S Q, Wu Y F, et al. Preparation of X-ray Fresnel zone plate by atomic layer deposition and focused ion beam slicing[J]. Acta Optica Sinica, 2023, 43(11): 1134001.

[7] 陶芬, 王玉丹, 任玉琦, 等. X射线纳米成像单毛细管椭球镜的设计与检测[J]. 光学学报, 2017, 37(10): 1034002.
Tao F, Wang Y D, Ren Y Q, et al. Design and detection of ellipsoidal mono-capillary for X-ray nano-imaging[J]. Acta Optica Sinica, 2017, 37(10): 1034002.

[8] Burcklen C, de Rossi S, Meltchakov E, et al. High-reflectance magnetron-sputtered scandium-based X-ray multilayer mirrors for the water window[J]. Optics Letters, 2017, 42(10): 1927-1930.

[9] 王国田, 王当笠, 曹健林, 等. 制备长波段X射线多层膜的新方法[J]. 应用光学, 2001, 22(6): 34-39.
Wang G T, Wang D L, Cao J L, et al. A new method of fabricating X-ray multilayer for long wavelength[J]. Journal of Applied Optics, 2001, 22(6): 34-39.

[10] Dixit S N. Numerical modeling of suppression of stimulated Brillouin scattering due to finite laser bandwidth[J]. Proceedings of SPIE, 1992, 1626: 254-265.

[11] Feng J T, Huang Q S, Qi R Z, et al. Stability of Cr/C multilayer during synchrotron radiation exposure and thermal annealing[J]. Optics Express, 2019, 27(26): 38493-38508.

[12] Wen M W, Huang Q S, Ma S, et al. Improvement of interface structure and polarization performance of Co/C multilayers by incorporation of nitrogen[J]. Optics Express, 2016, 24(24): 27166-27176.

[13] Qi R Z, Huang Q S, Fei J N, et al. Evolution of the internal structure of short-period Cr/V multilayers with different vanadium layers thicknesses[J]. Materials, 2019, 12(18): 2936.

[14] Huang Q S, Liu Y, Yang Y, et al. Nitridated Ru/B_4C multilayer mirrors with improved interface structure, zero stress, and enhanced hard X-ray reflectance[J]. Optics Express, 2018, 26(17): 21803-21812.

[15] Liu Y, Huang Q S, Qi R Z, et al. Microstructure evolution and hard X-ray reflectance of ultrathin Ru/C multilayer mirrors with different layer thicknesses[J]. Materials Research Express, 2021, 8(2): 026401.

[16] 廖珺晨, 钱芮, 陈冬, 等. GAZO/Ag/GAZO透明导电薄膜的磁控溅射制备及光电性能优化[J]. 激光与光电子学进展, 2023, 60(7): 0731002.
Liao J C, Qian R, Chen D, et al. Magnetron sputtering preparation and photoelectric property optimization of GAZO/Ag/GAZO transparent conductive thin films[J]. Laser & Optoelectronics Progress, 2023, 60(7): 0731002.

[17] 张云学, 黄秋实, 朱一帆, 等. 大尺寸高性能X射线双通道多层膜反射镜研制[J]. 光学学报, 2023, 43(2): 0234001.
Zhang Y X, Huang Q S, Zhu Y F, et al. Development of large-size high performance X-ray double-channel multilayer mirrors [J]. Acta Optica Sinica, 2023, 43(2): 0234001.

[18] Sechrist Z A, Fabreguette F H, Heintz O, et al. Optimization and structural characterization of W/Al_2O_3 nanolaminates grown using atomic layer deposition techniques[J]. Chemistry of Materials, 2005, 17(13): 3475-3485.

[19] Fabreguette F H, Wind R A, George S M. Ultrahigh X-ray reflectivity from W/Al_2O_3 multilayers fabricated using atomic layer deposition[J]. Applied Physics Letters, 2006, 88(1):

013116.

[20] 代敏. W/B_4C多层膜制备与表征的研究[D]. 长春: 长春理工大学, 2009: 6-8.
Dai M. Investigation on fabrication and measurement of W/B_4C multilayers[D]. Changchun: Changchun University of Science and Technology, 2009: 6-8.

[21] Parratt L G. Surface studies of solids by total reflection of X-rays [J]. Physical Review, 1954, 95(2): 359-369.

[22] Romaine S E, Everett J E, Bruni R J, et al. Characterization and multilayer coating of cylindrical x-ray optics for x-ray astronomy[J]. Proceedings of SPIE, 1998, 3444: 552-555.

[23] Spiller E, Rosenbluth A E. Determination of thickness errors and boundary roughness from the measured performance of A multilayer coating[J]. Optical Engineering, 1986, 25(8): 954-963.

[24] Suresh N, Phase D M, Gupta A, et al. Electron density fluctuations at interfaces in Nb/Si bilayer, trilayer, and multilayer films: an X-ray reflectivity study[J]. Journal of Applied Physics, 2000, 87(11): 7946-7958.

[25] Freitag J M, Clemens B M. Stress evolution in Mo/Si multilayers for high-reflectivity extreme ultraviolet mirrors[J]. Applied Physics Letters, 1998, 73(1): 43.

[26] Guo Q H, Shen J J, Du H M, et al. Structure and thermal stability of Mo/Al multilayers for soft X-ray mirrors[J]. Journal of Physics D: Applied Physics, 2005, 38(12): 1936-1942.

Preparation of X-Ray Multilayers Based on Atomic Layer Deposition

Lü Wensi[1,2], Wu Hongchang[1,3], Li Yanli[1*], Kong Xiangdong[1,2**], Han Li[1,2]

[1]*Institute of Electrical Engineering, Chinese Academy of Sciences, Beijing* 100190, *China*;

[2]*School of Electronic, Electrical, and Communication Engineering, University of Chinese Academy of Sciences, Beijing* 100049, *China*;

[3]*School of Physical Science and Technology, Lanzhou University, Lanzhou* 730000, *Gansu, China*

Abstract

Objective X-ray optical components are ones applied to the X-ray range and are widely employed in synchrotron radiation, free-electron lasers, high-energy astronomical observation, laboratory X-ray detection, and other scientific instruments. Among them, X-ray multilayers are important reflective optical components. Due to the short wavelength of X-rays, the multilayer period is usually in the order of a few to several tens of nanometres. In the case that the incident angle remains unchanged, the multilayer period decreases with the wavelength of X-rays. When the multilayer period is reduced to a few nanometres, the defects such as interface width and roughness will significantly reduce the X-ray reflectivity. Therefore, high-precision film preparation techniques are essential for fabricating X-ray multilayers with small periods. Several methods including ion beam sputtering, magnetron sputtering, and atomic layer deposition (ALD) have been adopted to prepare X-ray multilayers. Compared with other techniques, ALD shows advantages in achieving highly conformal films with precise control of film thicknesses on the order of angstroms. Thus, it has great potential for preparing multilayers with small periods. We study the preparation of an X-ray multilayer with small periods by the ALD method. Based on the film types that can be prepared by ALD, we calculate the X-ray (0.154 nm) reflectivity of four multilayers which consist of HfO_2/Al_2O_3, Ir/Al_2O_3, Ru/Al_2O_3, and W/Al_2O_3 respectively. We also further analyze the effects of the structural parameters of multilayers on the reflectivity including periodic thickness, duty ratios, and number of periods. Based on these results, the HfO_2/Al_2O_3 multilayer with period of 4 nm, number of periods of 60, and duty ratio of 0.5 is designed and prepared by ALD.

Methods In the theoretical part, we adopt the Fresnel coefficient recursion method to calculate the X-ray reflectivity of multilayers with different layer materials, periodic thickness, duty ratios, and number of periods. The influence of these parameters on the X-ray reflectivity is investigated. Based on the calculated results, the HfO_2/Al_2O_3 X-ray multilayer with periodic thickness of 4 nm, number of periods of 60, and duty ratio of 0.5 is designed. In the experimental part, ALD is applied to achieve HfO_2 and Al_2O_3 films. For each film, in a growth cycle, two reactants are employed as precursors and they react to form films on the substrate surface in a surface self-limiting growth mode. The film thickness is controlled by the cycle numbers. As for testing methods, ThermoFisher's Scios 2 dual-beam system is adopted to obtain a cross-section sample of the multilayer that is suitable for transmission electron microscope (TEM) observation. Meanwhile, the structure of the multilayer film is observed by JEOL JEM-2100F TEM. The X-ray reflectivity of the multilayer is tested on the Beijing synchrotron radiation 1W1A line station with an X-ray wavelength of 0.154 nm. Before the test, the multilayer is placed on a horizontal stage, and the positions of the sample stage and detector are adjusted. The data of X-ray intensity at different grazing angles are acquired and fitted by IMD software. The parameters and X-ray reflectivity of the multilayer are obtained from the fitted results accordingly.

Results and Discussions Figure 7 shows the TEM images of the cross-section of the HfO_2/Al_2O_3 multilayer at different magnifications. The interface between HfO_2 and Al_2O_3 is relatively sharp. However, the thickness of HfO_2 is slightly larger than that of Al_2O_3 in one period, which indicates that a small interdiffusion exists between the layers. The results of measured and fitted X-ray reflectivity of the HfO_2/Al_2O_3 multilayer are shown in Fig. 8. We find that two Bragg diffraction peaks appear at 1.15° and 2.23° respectively and the widths of the diffraction peaks are small, which reveals that the film deposition rate is stable and the thicknesses of each layer in the multilayer keep almost the same. By analyzing the fitted data, the X-ray reflectivity of the multilayer film is about 43%, which is a little lower than the theoretical value. The main reasons probably are the relatively large roughness of the Si substrate and the interdiffusion between the layers. For example, the roughness of the Si substrate can be transferred to the layers accumulatively, which leads to an increase in the scattering of X-rays and a decrease in the reflectivity.

Conclusions We study the preparation of X-ray multilayers by ALD technique. X-ray (0.154 nm) reflectivity of the multilayer in ideal conditions with different layer materials and structural parameters is calculated. Additionally, we also discuss the effects of layer materials, periodic thickness, duty ratios, and number of periods on the X-ray reflectivity in detail. The calculated results show that the X-ray reflectivity of HfO_2/Al_2O_3 multilayer with periodic thickness of 4 nm, duty ratio of 0.5, and number of periods of 60 is 53%. On this basis, the HfO_2/Al_2O_3 multilayer film is prepared by ALD. TEM results of the multilayer show a relatively sharp interface between the layers. X-ray reflectivity results indicate that the X-ray reflectivity of the multilayer is about 43%, which shows the great potential of the ALD method for preparing X-ray multilayers with small periods.

Key words atomic layer deposition; X ray; multilayer; reflectivity